Liu *et al. Chem Synth* 2024;4:31
DOI: 10.20517/cs.2023.70

Chemical Synthesis

Research Article

Open Access

Check for updates

Sustainable synthesis of Fe-MOR zeolite for efficient capture of CO_2

Pei Liu[1], Qinming Wu[1,2,*], Keping Yan[1,2], Liang Wang[1,2], Feng-Shou Xiao[1,2,*]

[1]College of Chemical and Biological Engineering, Zhejiang University, Hangzhou 310027, Zhejiang, China.
[2]Shanxi-Zheda Institute of Advanced Materials and Chemical Engineering, Taiyuan 030032, Shanxi, China.

[*]**Correspondence to:** Dr. Qinming Wu, Prof. Feng-Shou Xiao, College of Chemical and Biological Engineering, Zhejiang University, No. 866 Yuhangtang Road, Hangzhou 310027, Zhejiang, China. E-mail: qinmingwu@zju.edu.cn; fsxiao@zju.edu.cn

How to cite this article: Liu P, Wu Q, Yan K, Wang L, Xiao FS. Sustainable synthesis of Fe-MOR zeolite for efficient capture of CO_2. *Chem Synth* 2024;4:31. https://dx.doi.org/10.20517/cs.2023.70

Received: 26 Dec 2023 **First Decision:** 23 Apr 2024 **Revised:** 7 May 2024 **Accepted:** 27 May 2024 **Published:** 6 Jun 2024

Academic Editor: Jun Xu **Copy Editor:** Pei-Yun Wang **Production Editor:** Pei-Yun Wang

Abstract

Selective adsorption of carbon dioxide (CO_2) is significant for carbon neutrality, where searching for efficient CO_2 adsorbents is very important. In addition, coal fly ash (CFA) is one of the largest industrial solid wastes with environmental damages, where conversion of the wastes into costly functional materials is attractive. This work showed sustainable synthesis of Fe-containing mordenite (Fe-MOR) zeolite from the CFA waste under solvent-free conditions, and this zeolite is an efficient capturer for CO_2 in the mixture of CO_2/N_2 (15/85, v/v), giving adsorption capacity of 2.07 mmol/g and separation coefficient of 58.9 at 298 K. Very interestingly, the capture of CO_2 in the mixture of CO_2/N_2 (15/85, v/v) is recyclable. This work not only solved the accumulation and pollution of CFA but also prepared a highly efficient adsorbent of Fe-MOR zeolite, which would open a door for utilizing environmentally unfriendly solid wastes as value-added functional materials in the future.

Keywords: Sustainable synthesis, Fe-MOR zeolite, CO_2 capture, coal fly ash (CFA)

INTRODUCTION

The rapid increase of greenhouse gases, particularly carbon dioxide (CO_2), is one of the global problems that could increase the likelihood and severity of natural disasters such as wildfires, heatwaves, and droughts[1-8]. Since renewable energy resources are still being developed and thus fossil fuels will remain the dominant energy source for a long time, it is crucial to efficiently curb CO_2 emissions[9-17]. At present, great efforts have

been made in developing efficient technologies for capturing CO_2[18-22]. Among them, it is generally believed that solid porous adsorbents with low cost, high capacity and selectivity of CO_2 are critical.

Zeolites, as a class of typically solid porous adsorbents with ordered micropores, are widely employed in fields such as catalysis, ion exchange, adsorption, and separation due to their high surface areas, large micropore volumes, and good stabilities[23-26]. In recent years, capturing CO_2 by zeolites has become a hot topic due to their excellent stability for zeolite frameworks[3,4,18,27-32]. For example, Zhou *et al*. first reported that Fe-containing mordenite (Fe-MOR) zeolite synthesized from the "acid co-hydrolysis route" had narrowed microchannels, which was efficient for CO_2 adsorption and separation[33]. However, this method, which uses tetraethyl orthosilicate (TEOS) as a starting raw material and generates wastewater in the hydrothermal synthesis, incurs relatively high costs. In addition, conventional synthesis of Fe-MOR zeolite failed to obtain these narrowed microchannels under hydrothermal conditions due to the formation of aggregated Fe species. Thus, it is highly desirable to develop a simple and sustainable route for synthesizing Fe-MOR zeolite with high capacity and selectivity of CO_2.

Recently, we developed a simple and sustainable route for solvent-free synthesis of zeolites, which completely avoided using water solvents[34-38], where the aggregation of Fe species was effectively hindered[39]. Therefore, it offers the possibility of preparing Fe-containing zeolites without aggregation of Fe species under solvent-free conditions. Considering that coal fly ash (CFA), mainly containing silica, alumina, and iron oxides, one of the largest industrial solid wastes emitted from the combustion of coal powder, is environmentally unfriendly[40-45], it is really sustainable for the conversion of the CFA waste into highly efficient adsorbent of Fe-MOR zeolite under solvent-free conditions.

This work, for the first time, showed a simple and sustainable synthesis of Fe-MOR zeolite from CFA waste under solvent-free conditions. As expected, the Fe-MOR zeolite exhibited good adsorption capacity for CO_2 (2.07 mmol/g at 298 K), high separation coefficient (58.9 at 298 K), and excellent recyclability. These features, plus sustainable synthesis, are helpful for potential applications of this zeolite in the future.

EXPERIMENTAL

Solvent-free synthesis of Fe-MOR zeolite from CFA

Experimental sections, including materials and characterizations [Supplementary Materials].

For the solvent-free synthesis of Fe-MOR zeolite from CFA (Fe-MOR-CFA), the CFA and NaOH powder were mixed at a mass ratio of 1:1.2, calcined at 800 °C for 2 h, cooled to room temperature, and ground into a fine powder at room temperature[37]. The chemical composition of the CFA and the activated CFA by alkali fusion were measured with X-ray fluorescence (XRF) [Supplementary Table 1].

As a typical run for the solvent-free synthesis of Fe-MOR zeolite, 0.534 g of CFA fine powder, 0.879 g of solid silica, and 0.1 g of MOR zeolite as seeds were ground for 10 min. Subsequently, the obtained power was poured into an autoclave, and 1.2 g of H_2O was added. The product was finally crystallized at 175 °C for 10 h and designated as Fe-MOR-CFA. The yield of the Fe-MOR-CFA zeolite is approximately 90%. The Si/Al ratio and Fe content of the Fe-MOR-CFA zeolite were 6.9 and 0.77 wt.% by inductively coupled plasma optical emission spectroscopy (ICP-OES) measurements, which was consistent with the result of XRF [Supplementary Table 1].

For comparison, Fe-MOR zeolite was synthesized from an "acidic co-hydrolysis route" accordingly[33], which was designated as Fe-MOR-ACH. The Si/Al ratio and Fe content of the Fe-MOR-ACH zeolite were 6.5 and 0.73 wt.% by ICP-OES measurements.

Gas adsorption

Adsorption data for CO_2 and N_2 at 273 and 298 K were carried out in the Physical Adsorption Analyzer [Beishide Instrument Technology (Beijing) Co., Ltd., China]. Adsorption selectivity was based on ideal adsorbed solution theory (IAST)[33] for CO_2/N_2 (15/85, v/v), determined by:

$$S = \frac{x_i/x_j}{y_i/y_j} \quad (1)$$

Where x and y were the mole fraction of absorbate in the adsorption and gas phases, respectively. The subscripts i and j were on behalf of CO_2 and N_2.

Isosteric heat of adsorption[46] was calculated from the Clausius-Clapeyron equation to predict the interactions between the adsorbate and the adsorbent, using the CO_2 adsorption-desorption at 273 and 298 K, expressed as

$$In\ P = -\frac{\Delta H_s}{R \times T} + C \quad (2)$$

Where P was the pressure, R was the ideal gas constant, 8.314 kJ/mol, C was the constant, T was the temperature, K, and ΔH_s was calculated from slopes of plots of In P *vs.* $1/T$ of fixed loading.

The recyclability of single-component CO_2 adsorption was obtained on the Weight Method Vacuum Steam Absorption [Beishide Instrument Technology (Beijing) Co., Ltd., China].

CO_2 dynamic adsorption profiles for sole composition at 298 K were measured on the Gravity Vacuum Vapor Sorption Test Report [Beishide Instrument Technology (Beijing) Co., Ltd., China]. Firstly, 0.06~0.10 g of as-synthesized sample fine powder was loaded to the quartz tubing and activated under high vacuum at 573 K for 3 h. The pressure was increased to each set value (10, 20, 30, 40 kPa, *etc.*) at a rate of 10 kPa when the temperature cooled to 298 K. Each specific pressure was then maintained for a maximum of 3 h until adsorption equilibrium was reached.

The CO_2/N_2 breakthrough separations were performed in a multi-component adsorption breakthrough curve analyzer [Beishide Instrument Technology (Beijing) Co., Ltd., China] at 298 K. Firstly, 0.4~1.0 g of as-synthesized powder was placed in the quartz tubing (6 mm diameter) and then purged with He flow (5 mL/min) for 2 h at 573 K. The mixture (CO_2/N_2: 15/85, v/v) flows without water condition, with water condition and the presence of SO_2 (1,000 ppm) were then introduced at 3.0 mL/min at 298 K. The flow rates of all gas mixtures were regulated by mass flow controllers; the humidity was controlled and detected using a multi-component adsorption breakthrough curve analyzer, and the CO_2 and N_2 concentrations from the adsorbent bed were continuously monitored with a gas analytical mass spectrometer. Besides, the zeolite was regenerated *in situ* in the column with a 5 mL/min flow at 573 K for 2 h.

RESULTS AND DISCUSSION

Figure 1 displayed the schematic representation of solvent-free synthesis of Fe-MOR-CFA zeolite. Figure 2 showed the X-ray diffraction (XRD) pattern, scanning electron microscopy (SEM) image, N_2 sorption isotherms, and ^{27}Al magic-angle spinning (MAS) nuclear magnetic resonance (NMR) spectrum of Fe-MOR-CFA zeolite. The XRD pattern of the Fe-MOR-CFA zeolite [Figure 2A] displayed peaks with good resolution in the range of 5°-40°, which are well consistent with those of the simulated MOR structure

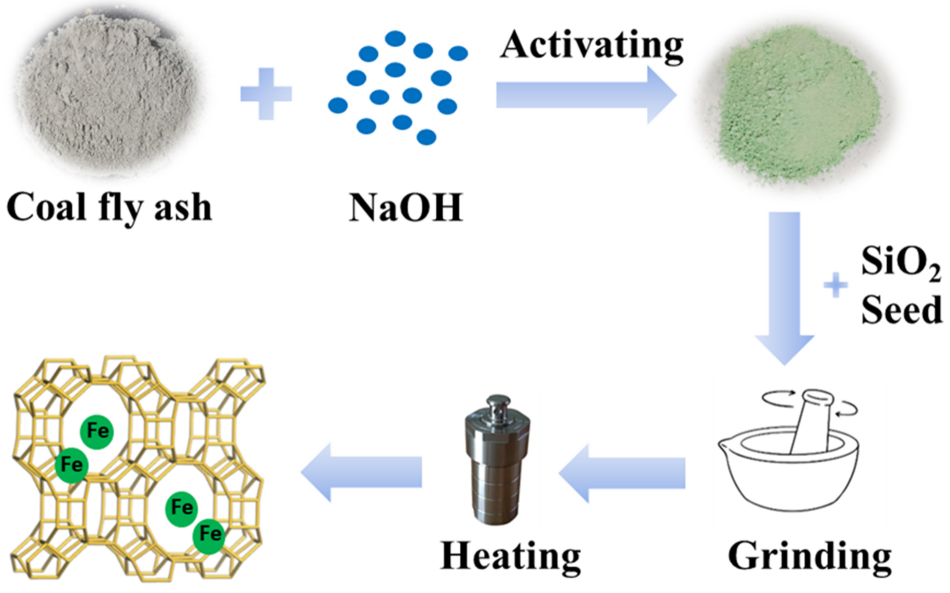

Figure 1. Schematic representation of solvent-free synthesis of Fe-MOR-CFA zeolite from coal fly ash. Fe-MOR-CFA: Fe-containing mordenite zeolite from coal fly ash.

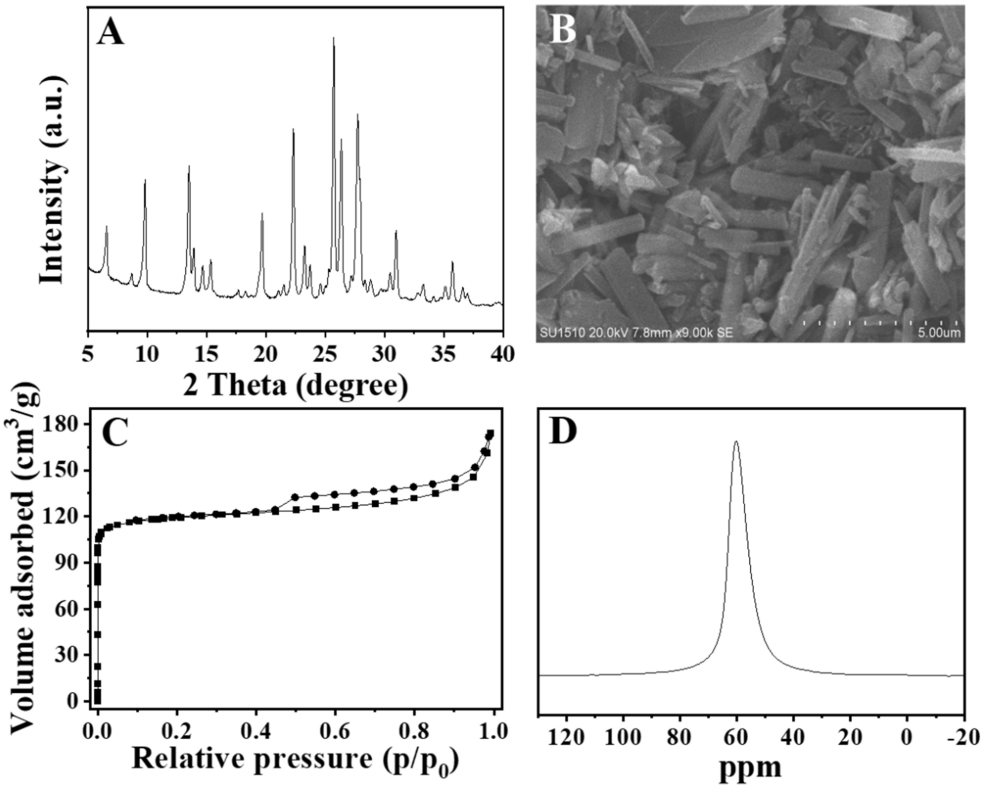

Figure 2. (A) XRD pattern; (B) SEM image; (C) N_2 sorption isotherms; and (D) ^{27}Al MAS NMR spectrum of the Fe-MOR-CFA zeolite. XRD: X-ray diffraction; SEM: scanning electron microscopy; MAS: ^{27}Al magic-angle spinning; NMR: nuclear magnetic resonance; Fe-MOR-CFA: Fe-containing mordenite zeolite from coal fly ash.

[Supplementary Figure 1] and Fe-MOR-ACH zeolite [Supplementary Figure 2]. The SEM image of the Fe-MOR-CFA zeolite [Figure 2B] showed rod-shaped morphology, which is very similar to that of Fe-MOR-ACH zeolite [Supplementary Figure 3]. The N_2 sorption isotherms of the H-Fe-MOR-CFA zeolite [Figure 2C] presented that the curve rose sharply at a relative pressure ($10^{-6} < P/P_0 < 0.01$) owing to the filling of as-synthesized zeolite micropores by N_2. Correspondingly, the Brunauer-Emmett-Teller (BET) surface area and micropore volume were 434 m^2/g and 0.18 cm^3/g, respectively, which are extremely similar to the conventional MOR zeolite synthesized from the conventional raw materials (BET surface area of 420 m^2/g, and micropore volume of 0.17 cm^3/g) and the Fe-MOR-ACH zeolite (BET surface area of 443 m^2/g and micropore volume of 0.18 cm^3/g) [Supplementary Figure 4][47]. Figure 2D displayed the ^{27}Al MAS NMR spectrum of the obtained Fe-MOR-CFA zeolite, giving a single peak with the chemical shift at about 60.4 ppm, which is commonly assigned to 4-coordinated Al species in the zeolite framework. After calcination at 823 K for 6 h, XRD patterns of Fe-MOR-CFA and Fe-MOR-ACH zeolites [Supplementary Figure 5] remained well, suggesting their good stabilities for the zeolite frameworks.

Ultraviolet-visible (UV-vis) and electron spin resonance (ESR) techniques were used to investigate the chemical state of Fe species. UV-vis spectra of the Fe-MOR-CFA and Fe-MOR-ACH zeolites displayed two monomer bands centered at 210-220 nm and 250-265 nm, respectively [Figure 3A]. The 210-220 nm band was assigned to tetrahedrally coordinated Fe^{3+} ions, while the 250-265 nm band was attributed to isolated Fe^{3+} ions with higher coordination[47,48]. Notably, no peaks between 300 and 400 nm in the Fe-MOR-CFA and Fe-MOR-ACH zeolites were associated with oligonuclear Fe_xO_y clusters[49]. Their ESR spectra [Figure 3B] exhibited the signal at g = 4.3 associated with isolated Fe^{3+} ions with tetrahedral coordination and the signal at g = 2.0 related to Fe species inside microporous channels[33,50]. The above results revealed that the aggregated Fe species were excluded in these zeolites, confirming the feasibility of solvent-free synthesis of Fe-MOR-CFA zeolite from CFA.

Supplementary Figures 6 and 7 exhibited the XRD patterns and SEM images of the Fe-MOR-CFA zeolite samples with different ratios of the MOR zeolite seeds to SiO_2 in the mixture of initial raw materials from 0 to 0.20. Notably, when no MOR zeolite seeds were added (a ratio of 0), the crystal size of the Fe-MOR-CFA zeolite was very large (with a diameter larger than 3 μm). However, when the zeolite seeds were included, the crystal sizes significantly decreased (with a diameter of less than 0.5 μm). These results suggested that a suitable ratio of the MOR zeolite seeds to SiO_2 is significant for adjusting zeolite crystal sizes.

Supplementary Figure 8 showed the effect of the Fe-MOR-CFA zeolite on the Na_2O/SiO_2 ratios in the mixture of initial raw materials. Pure Fe-MOR-CFA zeolite could be obtained when the ratios of Na_2O/SiO_2 were adjusted from 0.22 to 0.26 [Supplementary Figure 8A and B]. When the ratios were higher than 0.29, the ANA phase was observed in the zeolite product [Supplementary Figure 8C]. Therefore, the Na_2O/SiO_2 ratios should be seriously regulated in the solvent-free synthesis of the Fe-MOR-CFA zeolite.

Figure 4 showed the crystallization process of the Fe-MOR-CFA zeolite explored by XRD and SEM techniques. Firstly, very weak peaks of MOR zeolite before crystallization were observed, which was related to the MOR zeolite seeds in the mixture of initial raw materials [Figure 4A(a)]. A series of peaks associated with MOR structure appeared when the crystallization time was 4 h [Figure 4A(b)]. Meanwhile, a few Fe-MOR-CFA zeolite crystals could be observed obviously from the SEM image [Figure 4B(b)], which was extremely consistent with the XRD pattern. The zeolite crystals formed quickly from 4 to 6 h, as observed from both XRD patterns and SEM images [Figure 4A(c) and B(c)]. The XRD intensity of the obtained samples did not change after the crystallization for 10 h, meaning a full crystallization [Figure 4A(e)]. Accordingly, more Fe-MOR-CFA zeolite crystals could be attained [Figure 4B(e)]. The dependence of the

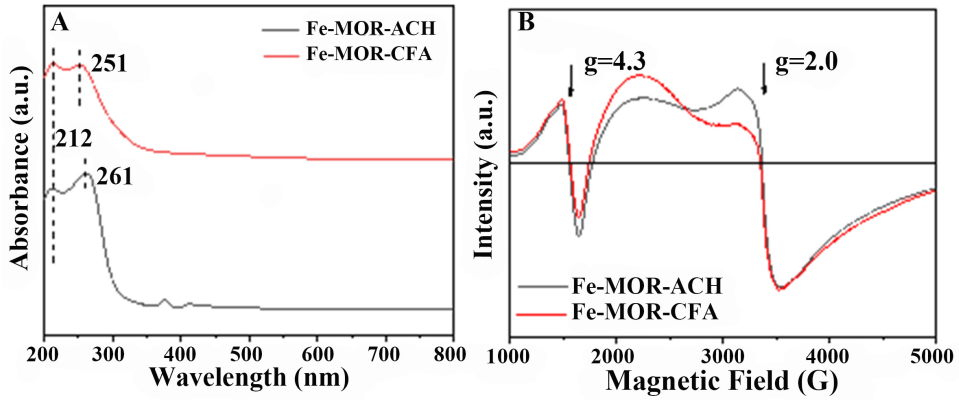

Figure 3. (A) UV-vis and (B) ESR spectra of Fe-MOR-CFA and Fe-MOR-ACH zeolites. UV-vis: Ultraviolet-visible; ESR: electron spin resonance; Fe-MOR-CFA: Fe-containing mordenite zeolite from coal fly ash; Fe-MOR-ACH: Fe-containing mordenite from acidic co-hydrolysis route.

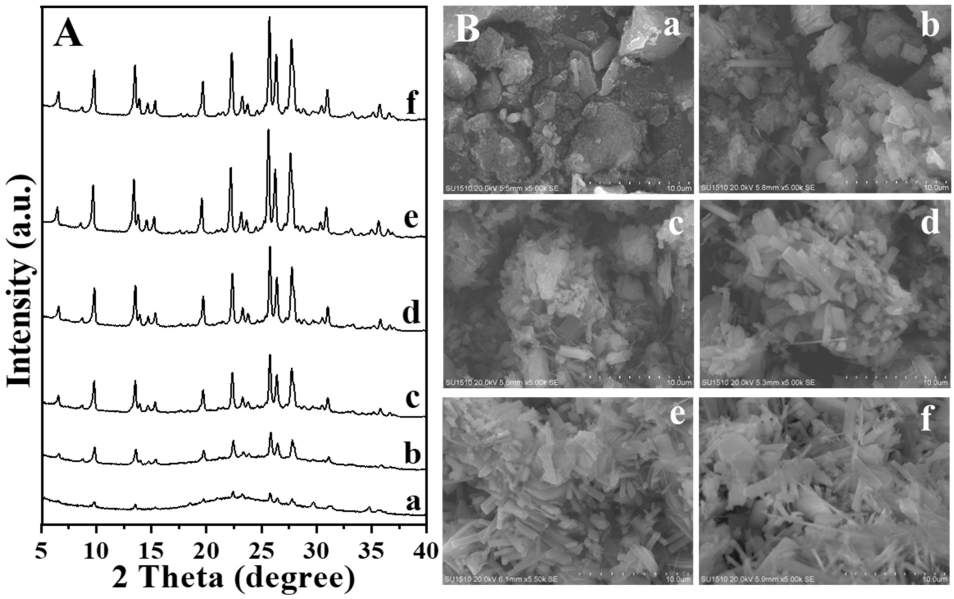

Figure 4. (A) XRD patterns and (B) SEM images of the Fe-MOR-CFA zeolite crystallized at (a) 0, (b) 4, (c) 6, (d) 8, (e) 10, and (f) 12 h, respectively. XRD: X-ray diffraction; SEM: scanning electron microscopy; Fe-MOR-CFA: Fe-containing mordenite zeolite from coal fly ash.

Fe-MOR-CFA zeolite crystallinity on crystallization time was shown in Supplementary Figure 9.

Quantitative porosity was analyzed using N_2 and Ar sorption experiments. Both the Fe-MOR-CFA and Fe-MOR-ACH zeolites exhibited extremely low N_2 and Ar uptake [Figure 5, Supplementary Figures 10 and 11, Supplementary Table 2], suggesting that both with narrowed orifices retard larger N_2 (3.64 Å) and even Ar (3.4 Å)[33]. In contrast, both samples enable CO_2 to enter with a small kinetic diameter (3.3 Å), as supported by CO_2 sorption isotherms of the samples [Figure 5]. The CO_2 adsorption capacities of the Fe-MOR-CFA zeolite at 273 and 298 K were 3.31 mmol/g and 2.93 mmol/g, respectively, which is comparable with those (3.45 and 3.09 mmol/g) of the Fe-MOR-ACH zeolite.

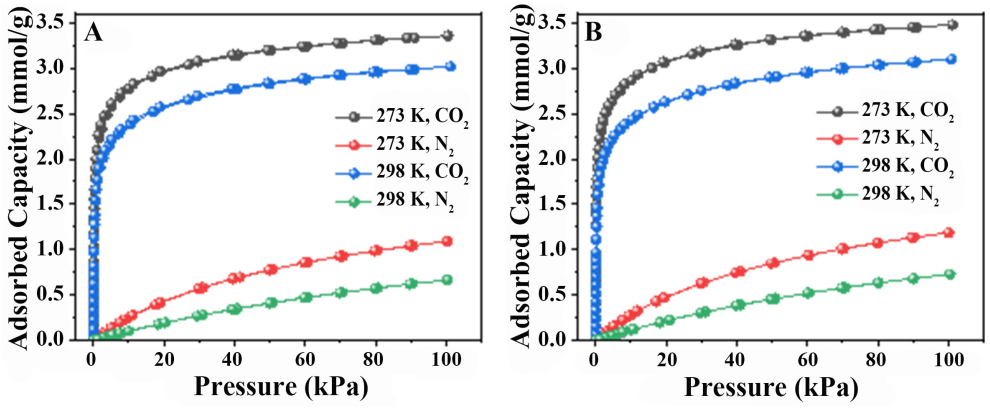

Figure 5. CO_2 and N_2 sorption isotherms of (A) Fe-MOR-CFA zeolite and (B) Fe-MOR-ACH zeolite at 273 and 298 K. Fe-MOR-CFA: Fe-containing mordenite zeolite from coal fly ash; Fe-MOR-ACH: Fe-containing mordenite from acidic co-hydrolysis route.

Figure 6A showed adsorption selectivity of CO_2/N_2 (15/85, v/v) calculated by single-component CO_2 and N_2 sorption isotherms at 273 and 298 K for Fe-MOR-CFA and Fe-MOR-ACH zeolites, giving excellent separation ability. Isosteric heats of CO_2 adsorption (Q_{st}) as a function of CO_2 uptakes were analyzed [Figure 6B], giving similar values for these two zeolites. In addition, they have similar CO_2 adsorption kinetics [Supplementary Figures 12 and 13], meaning similar electrostatic interaction between the iron species and CO_2[33,51]. After recycling ten times, no loss for CO_2 uptake at 298 K was observed for the Fe-MOR-CFA zeolite [Figure 6C], indicating its recyclability for adsorption and desorption of CO_2. Furthermore, the separation efficiency of the two zeolites was evaluated by the column breakthrough separations for the mixture of CO_2/N_2 (15/85, v/v) at 298 K and atmospheric pressure. As shown in Figure 6D, N_2 breakthrough occurred immediately, while the CO_2 retaining time of Fe-MOR-CFA and Fe-MOR-ACH zeolites were 100.4 and 97.0 min/g, respectively, and their CO_2 adsorption capacities were 2.07 and 2.02 mmol/g, respectively. From the breakthrough curve, the separation coefficient for Fe-MOR-CFA and Fe-MOR-ACH zeolites were calculated at 58.9 and 53.5 for CO_2/N_2 (15/85, v/v), respectively, where the Fe-MOR-CFA zeolite exhibited the separation coefficient even better than Fe-MOR-ACH zeolite, one of the best zeolite adsorbents of CO_2 yet. The better performance might be associated with K^+ and Ca^{2+} in the raw materials (CFA)[52]. In addition, the column breakthrough separations of the Fe-MOR-CFA zeolite with a relative humidity (RH) of 60% and the presence of SO_2 (1,000 ppm) were performed at 298 K [Supplementary Figure 14]. The results showed the CO_2 retaining time at 99.8 and 97.0 min/g, the CO_2 adsorption capacity at 2.08 and 2.02 mmol/g, and the separation coefficient at 58.0 and 56.7, respectively. These results indicate that the Fe-MOR-CFA zeolite has excellent tolerance to water and SO_2. Moreover, the recyclability tests under the mixture of CO_2/N_2 (15/85, v/v) at 298 K also demonstrate the excellent long-term stability and performance over extended cycles of the Fe-MOR-CFA zeolite [Supplementary Figure 15 and Supplementary Table 3]. Subsequently, the column breakthrough separation for the mixture of CO_2/N_2 (50/50, v/v) over the Fe-MOR-CFA zeolite was conducted at 298 K [Supplementary Figure 16], confirming that the Fe-MOR-CFA zeolite had excellent CO_2 adsorption performance with the CO_2 retaining time of 34.6 min/g, the CO_2 adsorption capacity of 2.40 mmol/g, and the separation coefficient of 44.0.

Finally, the solvent-free synthesis of the Fe-MOR-CFA zeolite was scaled up to 100-200 mL autoclaves [Supplementary Figure 17]. The obtained zeolites showed high crystallinity and rod-shaped morphology [Supplementary Figures 18 and 19]. Moreover, the column breakthrough separations of the products for the mixture of CO_2/N_2 (15/85, v/v) showed that these products still owned excellent CO_2 adsorption performance, giving the CO_2 retaining time at 102.9-104.3 min/g and the CO_2 adsorption capacity at 2.07-2.10 mmol/g [Supplementary Figure 20]. Particularly, the cost of these products in this work is lower by at least 50% than that of conventional products.

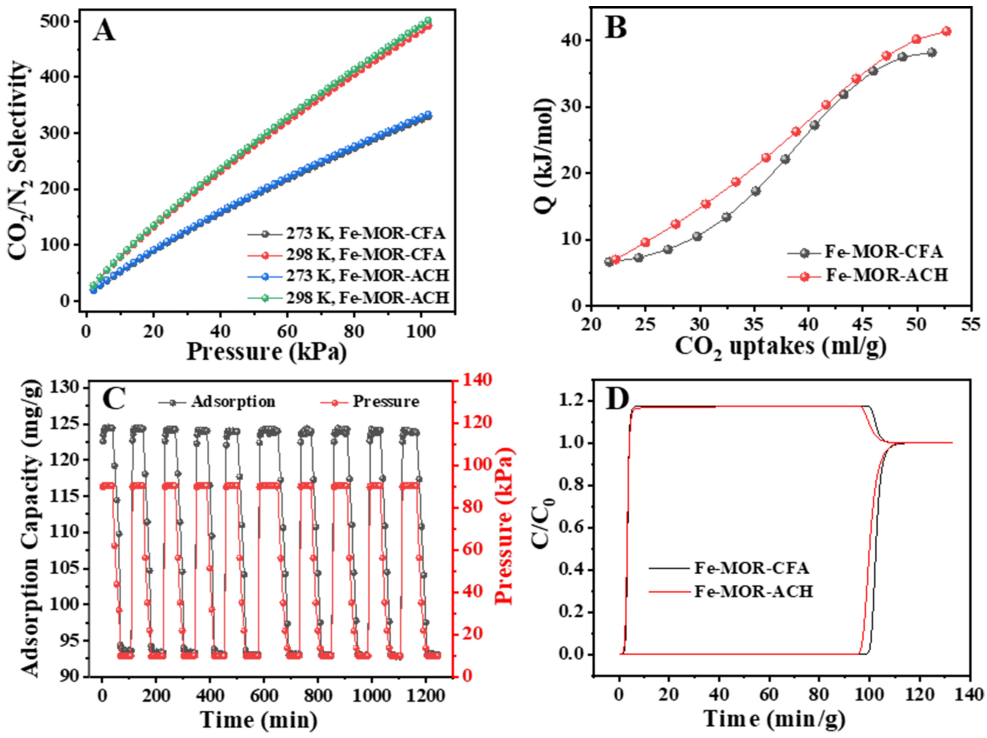

Figure 6. (A) IAST prediction of CO_2/N_2 (15/85, v/v) selectivities on Fe-MOR-CFA zeolite and Fe-MOR-ACH zeolite at 273 and 298 K; (B) Isosteric heats (Q_{st}) as a function of CO_2 uptakes on Fe-MOR-CFA zeolite and Fe-MOR-ACH zeolite; (C) CO_2 adsorption isotherms of Fe-MOR-CFA zeolite for ten times at 298 K; (D) Experimental column breakthrough curves for CO_2/N_2 (15/85, v/v) separations on Fe-MOR-CFA zeolite and Fe-MOR-ACH zeolite at 298 K. IAST: Ideal adsorbed solution theory; Fe-MOR-CFA: Fe-containing mordenite zeolite from coal fly ash; Fe-MOR-ACH: Fe-containing mordenite from acidic co-hydrolysis route.

CONCLUSIONS

In summary, it is successful for solvent-free synthesis of Fe-MOR-CFA zeolite with high yields using solid waste of CFA as aluminum, silicon, and iron sources. This route not only consumes solid waste of CFA but also produces value-added CO_2 adsorbents with high adsorption capacity, excellent separation coefficient, and good recyclability. The sustainable synthesis plus excellent features for capturing CO_2 could provide a good opportunity for potential applications of the Fe-MOR-CFA zeolite in the future.

DECLARATIONS

Acknowledgments

We sincerely thank all the team members who participated in this study.

Authors' contributions

Zeolite preparation, characterization, and the draft manuscript: Liu P
Discussion on the results: Yan K, Wang L
Design of the study, data analysis, and manuscript writing: Wu Q, Xiao FS

Availability of data and materials

Not applicable.

Financial support and sponsorship

This work was supported by the National Key Research and Development Program of China (2022YFA1503602), Shanxi-Zheda Institute of Advanced Materials and Chemical Engineering (2021SZ-AT003), and the National Natural Science Foundation of China (22288101 and 22172141).

Conflicts of interest

Wang L is the Junior Editorial Board Member of *Chemical Synthesis*. Both Wang L and Xiao FS are the guest editors of the Special Issue of "Zeolite for Sustainable Catalysis", while the other authors have declared that they have no conflicts of interest.

Ethical approval and consent to participate

Not applicable.

Consent for publication

Not applicable.

REFERENCES

1. Varghese AM, Karanikolos GN. CO_2 capture adsorbents functionalized by amine - bearing polymers: a review. *Int J Greenh Gas Con* 2020;96:103005. DOI
2. Singh G, Lee J, Karakoti A, et al. Emerging trends in porous materials for CO_2 capture and conversion. *Chem Soc Rev* 2020;49:4360-404. DOI PubMed
3. Siegelman RL, Kim EJ, Long JR. Porous materials for carbon dioxide separations. *Nat Mater* 2021;20:1060-72. DOI PubMed
4. Osman AI, Hefny M, Abdel Maksoud MIA, Elgarahy AM, Rooney DW. Recent advances in carbon capture storage and utilisation technologies: a review. *Environ Chem Lett* 2021;19:797-849. DOI
5. Liu X, Wang M, Zhou C, et al. Selective transformation of carbon dioxide into lower olefins with a bifunctional catalyst composed of $ZnGa_2O_4$ and SAPO-34. *Chem Commun* 2018;54:140-3. DOI PubMed
6. Lashaki M, Khiavi S, Sayari A. Stability of amine-functionalized CO_2 adsorbents: a multifaceted puzzle. *Chem Soc Rev* 2019;48:3320-405. DOI PubMed
7. Kolle JM, Fayaz M, Sayari A. Understanding the effect of water on CO_2 adsorption. *Chem Rev* 2021;121:7280-345. DOI PubMed
8. Hu Z, Wang Y, Shah BB, Zhao D. CO_2 capture in metal–organic framework adsorbents: an engineering perspective. *Adv Sustain Syst* 2019;3:1800080. DOI
9. Song C, Liu Q, Deng S, Li H, Kitamura Y. Cryogenic-based CO_2 capture technologies: state-of-the-art developments and current challenges. *Renew Sustain Energy Rev* 2019;101:265-78. DOI
10. Shehzad N, Tahir M, Johari K, Murugesan T, Hussain M. A critical review on TiO_2 based photocatalytic CO_2 reduction system: strategies to improve efficiency. *J CO2 Util* 2018;26:98-122. DOI
11. Nikoloudakis E, López-Duarte I, Charalambidis G, Ladomenou K, Ince M, Coutsolelos AG. Porphyrins and phthalocyanines as biomimetic tools for photocatalytic H_2 production and CO_2 reduction. *Chem Soc Rev* 2022;51:6965-7045. DOI PubMed
12. Muhammed NS, Haq B, Al Shehri D, Al-ahmed A, Rahman MM, Zaman E. A review on underground hydrogen storage: insight into geological sites, influencing factors and future outlook. *Energy Rep* 2022;8:461-99. DOI
13. Fan WK, Tahir M. Recent advances on cobalt metal organic frameworks (MOFs) for photocatalytic CO_2 reduction to renewable energy and fuels: a review on current progress and future directions. *Energ Convers Manage* 2022;253:115180. DOI
14. Du Z, Liu C, Zhai J, et al. A review of hydrogen purification technologies for fuel cell vehicles. *Catalysts* 2021;11:393. DOI
15. Dissanayake PD, You S, Igalavithana AD, et al. Biochar-based adsorbents for carbon dioxide capture: a critical review. *Renew Sustain Energy Rev* 2020;119:109582. DOI
16. Chakraborty R, K V, Pradhan M, Nayak AK. Recent advancement of biomass-derived porous carbon based materials for energy and environmental remediation applications. *J Mater Chem A* 2022;10:6965-7005. DOI
17. Chai Y, Gao N, Wang M, Wu C. H_2 production from co-pyrolysis/gasification of waste plastics and biomass under novel catalyst Ni-CaO-C. *Chem Eng J* 2020;382:122947. DOI
18. Tawalbeh M, Muhammad Nauman Javed R, Al-othman A, Almomani F. The novel contribution of non-noble metal catalysts for intensified carbon dioxide hydrogenation: recent challenges and opportunities. *Energ Convers Manage* 2023;279:116755. DOI
19. Pal S, Krishna R, Das MC. Highly scalable acid-base resistant Cu-Prussian blue metal-organic framework for C_2H_2/C_2H_4, biogas, and flue gas separations. *Chem Eng J* 2023;460:141795. DOI

20. Jiang L, Liu W, Wang R, et al. Sorption direct air capture with CO_2 utilization. *Prog Energ Combust* 2023;95:101069. DOI
21. Hu Y, Jiang Y, Li J, et al. New-generation anion-pillared metal–organic frameworks with customized cages for highly efficient CO_2 capture. *Adv Funct Mater* 2023;33:2213915. DOI
22. Ding H, Zhang Y, Dong Y, Wen C, Yang Y. High-pressure supersonic carbon dioxide (CO_2) separation benefiting carbon capture, utilisation and storage (CCUS) technology. *Appl Energy* 2023;339:120975. DOI
23. Zhou H, Yi X, Hui Y, et al. Isolated boron in zeolite for oxidative dehydrogenation of propane. *Science* 2021;372:76-80. DOI PubMed
24. Xiong H, Liu Z, Chen X, et al. In situ imaging of the sorption-induced subcell topological flexibility of a rigid zeolite framework. *Science* 2022;376:491-6. DOI PubMed
25. Tai W, Dai W, Wu G, Li L. A simple strategy for synthesis of *b*-axis-oriented MFI zeolite macro-nanosheets. *Chem Synth* 2023;3:38. DOI
26. Yuan K, Jia X, Wang S, et al. Effect of crystal size of ZSM-11 zeolite on the catalytic performance and reaction route in methanol to olefins. *Chem Synth* 2023;4:31. DOI
27. Sun Y, Lang Q, Fu G, et al. Highly hydrophobic zeolite ZSM-8 with perfect framework structure obtained in a strongly acidic medium. *Micropor Mesopor Mat* 2024;363:112839. DOI
28. Jalali A, Ahmadpour A, Ghahramaninezhad M, Yasari E. Hierarchical nanocomposites derived from UiO-66 framework and zeolite for enhanced CO_2 adsorption. *J Environ Chem Eng* 2023;11:111294. DOI
29. Najafi AM, Khorasheh F, Soltanali S, Ghassabzadeh H. Equilibrium and kinetic insights into the comprehensive investigation of CO_2, CH_4, and N_2 adsorption on cation-exchanged X and Y faujasite zeolites. *Langmuir* 2023;39:15535-46. DOI PubMed
30. Kencana KS, Choi HJ, Kemp KC, Hong SB. Enhancing the CO_2 adsorption kinetics on Na-RHO and Cs-MER zeolites by NH_4F/H_2O_2 etching induced mesoporosity. *Chem Eng J* 2023;451:138520. DOI
31. Jiang Y, Zhou W, He N, Yan S, Chen S, Liu J. Preparation of shaped binder-free SSZ-13 zeolite and its application in CO_2 adsorption and catalysis. *ChemCatChem* 2022;14:e202200795. DOI
32. Fu D, Park Y, Davis ME. Confinement effects facilitate low-concentration carbon dioxide capture with zeolites. *Proc Natl Acad Sci U S A* 2022;119:e2211544119. DOI PubMed PMC
33. Zhou Y, Zhang J, Wang L, et al. Self-assembled iron-containing mordenite monolith for carbon dioxide sieving. *Science* 2021;373:315-20. DOI PubMed
34. Wu Q, Meng X, Gao X, Xiao FS. Solvent-free synthesis of zeolites: mechanism and utility. *Acc Chem Res* 2018;51:1396-403. DOI PubMed
35. Wu Q, Ma Y, Wang S, Meng X, Xiao F. *110th Anniversary:* sustainable synthesis of zeolites: from fundamental research to industrial production. *Ind Eng Chem Res* 2019;58:11653-8. DOI
36. Ma Y, Han S, Wu Q, et al. One-pot fabrication of metal-zeolite catalysts from a combination of solvent-free and sodium-free routes. *Catal Today* 2021;371:64-8. DOI
37. Liu P, Wu Q, Yan K, Wang L, Xiao FS. Solvent-free synthesis of FAU zeolite from coal fly ash. *Dalton Trans* 2022;52:24-8. DOI PubMed
38. Kan X, Xiao S, Zheng Y, et al. Sustainable synthesis of ordered mesoporous materials without additional solvents. *J Colloid Interface Sci* 2022;619:116-22. DOI PubMed
39. Ren L, Wu Q, Yang C, et al. Solvent-free synthesis of zeolites from solid raw materials. *J Am Chem Soc* 2012;134:15173-6. DOI PubMed
40. Qian B, Zhang J, Zhou S, et al. Synthesis of (111) facet-engineered MgO nanosheet from coal fly ash and its superior catalytic performance for high-temperature water gas shift reaction. *Appl Catal A Gen* 2021;618:118132. DOI
41. Park S, Kim M, Lim Y, et al. Characterization of rare earth elements present in coal ash by sequential extraction. *J Hazard Mater* 2021;402:123760. DOI PubMed
42. Guan Q, Hu X, Wu D, Shang X, Ye C, Kong H. Phosphate removal in marine electrolytes by zeolite synthesized from coal fly ash. *Fuel* 2009;88:1643-9. DOI
43. Yamaura M, Fungaro DA. Synthesis and characterization of magnetic adsorbent prepared by magnetite nanoparticles and zeolite from coal fly ash. *J Mater Sci* 2013;48:5093-101. DOI
44. Tauanov Z, Tsakiridis PE, Mikhalovsky SV, Inglezakis VJ. Synthetic coal fly ash-derived zeolites doped with silver nanoparticles for mercury (II) removal from water. *J Environ Manage* 2018;224:164-71. DOI PubMed
45. Bukhari SS, Behin J, Kazemian H, Rohani S. Conversion of coal fly ash to zeolite utilizing microwave and ultrasound energies: a review. *Fuel* 2015;140:250-66. DOI
46. You J, Wang H, Xiao T, Wu X, Zhang L, Lu C. Introducing high concentration of hexafluorosilicate anions into an ultra-microporous MOF for highly efficient C_2H_2/CO_2 and C_2H_2/C_2H_4 separation. *Chem Eng J* 2023;477:147001. DOI
47. Yasumura S, Qian Y, Kato T, et al. *In situ*/*operando* spectroscopic studies on the NH_3–SCR mechanism over Fe–zeolites. *ACS Catal* 2022;12:9983-93. DOI
48. Romero-sáez M, Divakar D, Aranzabal A, González-velasco J, González-marcos J. Catalytic oxidation of trichloroethylene over Fe-ZSM-5: influence of the preparation method on the iron species and the catalytic behavior. *Appl Catal B Environ* 2016;180:210-8. DOI
49. Zeng J, Chen S, Fan Z, Wang C, Chang H, Li J. Simultaneous selective catalytic reduction of NO and N_2O by NH_3 over Fe-zeolite

catalysts. *Ind Eng Chem Res* 2020;59:19500-9. DOI

50. Lari GM, Mondelli C, Pérez-ramírez J. Gas-phase oxidation of glycerol to dihydroxyacetone over tailored iron zeolites. *ACS Catal* 2015;5:1453-61. DOI
51. Liang L, Liu C, Jiang F, et al. Carbon dioxide capture and conversion by an acid-base resistant metal-organic framework. *Nat Commun* 2017;8:1233. DOI PubMed PMC
52. Najafi AM, Soltanali S, Ghassabzadeh H. Enhancing the CO_2, CH_4, and N_2 adsorption and kinetic performance on FAU zeolites for CO_2 capture from flue gas by metal incorporation technique. *Chem Eng J* 2023;468:143719. DOI